

UNIVERSITY OF CALIFORNIA - BERKELEY

UCRL-1261

C.2

TWO-WEEK LOAN COPY

*This is a Library Circulating Copy
which may be borrowed for two weeks.
For a personal retention copy, call
Tech. Info. Division, Ext. 5545*

RADIATION LABORATORY

UCRL-1261
C.2

DISCLAIMER

This document was prepared as an account of work sponsored by the United States Government. While this document is believed to contain correct information, neither the United States Government nor any agency thereof, nor the Regents of the University of California, nor any of their employees, makes any warranty, express or implied, or assumes any legal responsibility for the accuracy, completeness, or usefulness of any information, apparatus, product, or process disclosed, or represents that its use would not infringe privately owned rights. Reference herein to any specific commercial product, process, or service by its trade name, trademark, manufacturer, or otherwise, does not necessarily constitute or imply its endorsement, recommendation, or favoring by the United States Government or any agency thereof, or the Regents of the University of California. The views and opinions of authors expressed herein do not necessarily state or reflect those of the United States Government or any agency thereof or the Regents of the University of California.

The Energy Spectrum of the Positrons from Mu-Meson Decay

By

William Lester Gardner, Jr.
A.B. (Xavier University, Cincinnati) 1942

May 1951

DISSERTATION

Submitted in partial satisfaction of the requirements for the degree of

DOCTOR OF PHILOSOPHY

in

Physics

in the

GRADUATE DIVISION

of the

UNIVERSITY OF CALIFORNIA

Approved:

.....
.....
.....

Committee in Charge

Deposited in the University Library.....
Date Librarian

TABLE OF CONTENTS

	Page
I INTRODUCTION	3
A. Background and History	3
B. General Outline of the Experiment	5
II APPARATUS	7
A. Spiral Orbit Spectrometer	7
B. Scintillation Detection of Particles	12
C. Electronic Circuits	12
D. Background Determination	13
E. Operational Procedure	14
III EXPERIMENTAL RESULTS	16
IV ACCURACY OF THE MEASUREMENTS	17
A. Magnetic Field and Orbit Determinations	17
B. Evaluation of Additional Background Effects and Energy Corrections	17
1. Energetic Beta-Rays	18
2. Electrons from μ -Decay	19
3. First Crystal as Source of Positrons	19
4. Scattering of Electrons	19
5. Energy Loss	20
6. Miscellaneous Sources	21
C. Resolution Curve of Spectrometer	21
V MESON DECAY PROCESS AND OUTLINE OF MESON THEORIES	24
VI CONCLUSIONS	27
VII ACKNOWLEDGMENTS	30

I INTRODUCTION

A. History and Background

The existence of mesons was predicted by Yukawa in 1935 and these most recent additions to the elementary particles of physics were first observed by Anderson in 1937. Cosmic rays were the first and for many years the only available source of these mesons. Notwithstanding the low intensity of this source, many of the fundamental properties of the mesons were defined in very striking experiments.

Conversi, Pancini, and Piccioni¹ by deflecting the incoming cosmic-ray particles in a magnetic field obtained evidence which suggested more than one type of meson. Soon thereafter Lattes, Muirhead, Occhialini, and Powell² established the existence of two species of mesons by observing events in nuclear emulsions wherein a π^- (heavy) meson decayed into a μ^- (light) meson. They were also able to determine that the ratio of the masses m_π/m_μ would be about 1.5. An early determination of the mass of the μ -meson by its range and curvature in a cloud chamber was made by Fretter³ and he arrived at a value of about 200 electron masses. Cloud chamber evidence also indicated the charge of the mesons to be the electronic charge e .

With the availability of high energy accelerators as a source of mesons, many more of the meson characteristics have become known. π -mesons are produced in high energy beams, and are the mesons which have the strongest interactions with nuclei. μ -mesons appear to be created only in a decay process of the π , and they react only weakly

¹ Conversi, Pancini, and Piccioni, Phys. Rev. 71, 209 (1947)

² Lattes, Muirhead, Occhialini, and Powell, Nature 159, 694 (1947)

³ W. Fretter, Phys. Rev. 70, 625 (1946)

with nuclei. In the present experiment, only the positive mesons are of interest, and experimental data indicate that the decay scheme is as follows: π^+ -mesons stopping in matter undergo $\pi^+ \rightarrow \mu^+ + \text{neutrino}$ decay with a mean life of 2.6×10^{-8} sec.⁴ The μ^+ -mesons are monoenergetic, with an energy close to 4 Mev. The μ^+ -meson in turn decays with the characteristic mean life of 2.15×10^{-6} sec.^{5,6} The μ^+ -meson decay of $\mu^+ \rightarrow e^+ + 2 \text{ neutrinos}$ as will be discussed in a later section, is the most generally accepted process, and the entire decay scheme might be summarized as follows:

$$\pi^+ \rightarrow \mu^+ + \nu \quad (\tau = 2.6 \times 10^{-8})$$

$$\mu^+ \rightarrow e^+ + 2\nu \quad (\tau = 2.15 \times 10^{-6})$$

The positrons of the μ^+ -meson decay have energies up to the region of 55 Mev, and it is the spectrum of these energies that we are concerned with.

Previous investigations of this positron spectrum have employed various methods, but all have one point in common -- the use of cosmic-ray mesons as a source. The method of Steinberger⁷ involved absorption of the positrons, i.e. a range analysis. This is a difficult approach because of the large straggling of the positrons of this momentum range. Leighton, Anderson, and Seriff,⁸ employing a cloud chamber in a magnetic field, obtained 75 pictures of μ decay particles, both electrons and positrons. This small number of points when spread out over the energy

⁴ O. Chamberlain, R. Mozeley, J. Steinberger, C. Wiegand, Phys. Rev. 79 394 (1950)

⁵ N. Nereson and E. Rossi, Phys. Rev. 64, 199 (1943)

⁶ L. Alvarez, A. Longacre, V. Ogren, R. Thomas, Phys. Rev. 77, 752A (1950)

⁷ J. Steinberger, Phys. Rev. 75, 1136 (1949)

⁸ R. Leighton, C. Anderson, A. Seriff, Phys. Rev. 75, 1432 (1949)

spectrum result in an appreciable probable error in the final curve. Another investigation, conducted by Davis, Lock, and Muirhead,⁹ used the relationship between the mean square scattering angle and the energy of the particles. This method is subject to the large fluctuations of scattering, and the difficulties of the measurements in an emulsion.

B. General Outline of the Experiment

An investigation of the energy of the electrons resulting from the decay of μ -mesons has been conducted using a relatively new technique. Mesons produced artificially by protons from the 184-inch cyclotron are used as the source of positrons, and the energies of these positrons are measured in a "Spiral Orbit Spectrometer."

This type of spectrometer has been studied and developed in Japan¹⁰ since 1940. The spectrometer employed in this experiment embodies the principles learned in those studies, and is constructed on a somewhat larger scale than any of its prototypes.

The combination of the cyclotron beam and the Spiral Orbit Spectrometer has enabled us to conduct a controlled experiment on the energy spectrum. The relatively high counting rate and energy resolution permit a considerable extension in the accuracy of the spectrum as given by previous research.^{7,8,9} This accuracy will be of appreciable assistance in the consideration of various meson theories and their correlation with μ -meson decay. The precision of measurement of the

⁹ J. Davis, W. Lock, H. Muirhead, Phil. Mag. 40, 1250 (1949)

¹⁰ G. Miyamoto, Proc. Phys. Math. Soc. Jap. (1942)
Proc. Phys. Soc. Jap. 17, 587 (1943)
M. Sakai, J. Phys. Soc. Jap. 5, 178 (1950)

energy also opens up the possibility of an accurate and distinctly different approach to the mass of the μ -meson.

The external deflected beam of 340 Mev protons from the cyclotron produces π -mesons of both + and - variety. We are interested primarily in the π^+ -meson production. The cross section for π^+ production by protons, and energy loss of the π^+ , in various elements has been investigated by Richman¹¹ and others. Within the limitations of the spectrometer, the target is designed to make maximum use of the known data. The target of the cyclotron beam is located at the source position of the spectrometer. π^+ -mesons which stop in the target give rise to μ^+ -mesons through the $\pi^+ \rightarrow \mu^+ + \nu$ decay process. The 4 Mev energy of the μ^+ -meson is absorbed in approximately 0.2 gram/cm² of carbon and therefore almost all of the mesons remain in the target. Their decay gives rise to the positrons, and the magnetic field of the spectrometer is employed to define a particular energy interval of the energy spectrum present. The positrons are detected by four scintillations crystals and associated photomultiplier tube in quadruple coincidence.

¹¹ C. Richman and H. Wilcox. Phys. Rev. 78, 85A (1950)

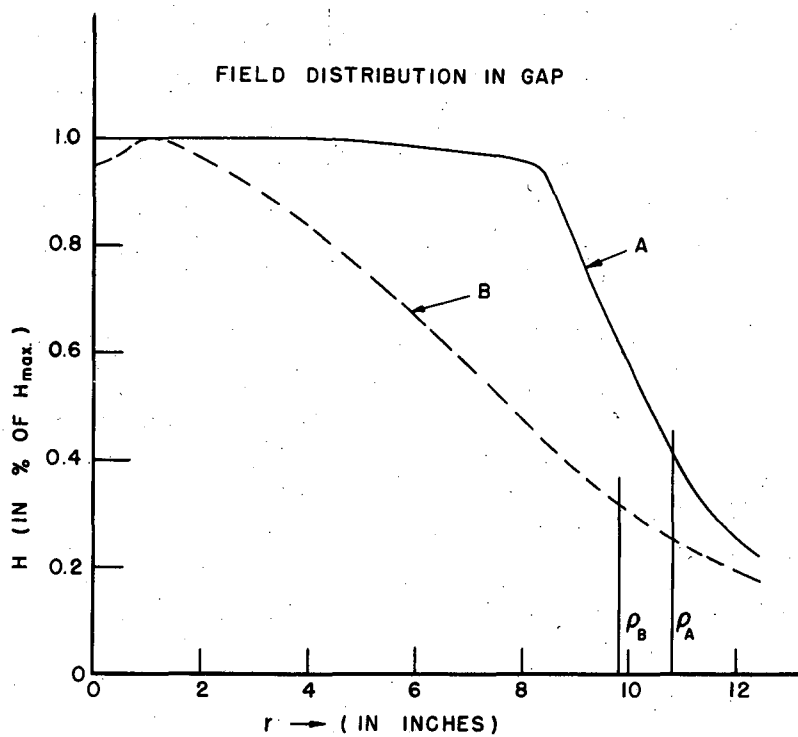
II APPARATUS

A. Spiral Orbit Spectrometer

The "Spiral Orbit" spectrometer has been given this name because of the manner in which the particles of a particular momentum, emerging from the center, spiral outward and approach the so-called "stable orbit." Particles of a lower momentum will be turned back before reaching the orbit, and will return to the origin. Particles of a higher momentum will go out, pass through the orbit, and be lost. The rapidity with which a particle of the correct momentum reaches the orbit is of course dependent on the particular magnetic field distribution employed. For a field distribution similar to that labeled "B" in Figure 1 it has been demonstrated¹⁰ that a particle of a momentum to be focused in the orbit is already close to the orbit after it has turned through less than 180° from its original angle of emission. And, a particle of momentum only 10 percent lower will have a maximum travel out from the center of less than $6/10$ of the radius to the orbit, and is then deflected back to the origin. A critical stability exists for particles in the "stable" orbit. After a few traversals of the circular orbit they eventually are lost.

An outstanding advantage of this type of spectrometer is that it focuses particles emerging in any direction from the center, confining our discussion to the median plane. This feature combined with a relatively large vertical focusing (that is, along the z direction) results in a large "luminosity" or transmission coefficient, which is always a figure of prime importance in a beta-ray spectrometer.

Let the axis of symmetry of the magnetic field be coincident with the axis of cylindrical coordinates, and take the median plane of the



MU 1807

Figure 1. Magnetic field distribution in gap.

pole gap as the plane $z = 0$. Then the magnetic field equations are

$$H_r = H_r(r, z) = -H_r(r, -z)$$

$$H_\theta = 0$$

$$H_z = H_z(r, z) = H_z(r, -z)$$

Except for the incremental change in magnetic field setting when a different momentum interval of the positron flux is being observed -- the magnetic field of the spectrometer is constant in time.

It might be of advantage to employ the Vector Potential A wherein

$$H_r = -\frac{\partial A}{\partial z} \quad H_\theta = 0 \quad H_z = \frac{1}{r} \frac{\partial}{\partial r} (rA)$$

and $A(z, r) = A(-z, r)$, since the plane $z = 0$ is a plane of symmetry.

Then the motion of a charged particle of charge $-e$ and mass m can be expressed as follows:

$$\frac{d\bar{p}}{dt} = -e \left(\frac{d\bar{r}}{dt} \times \bar{H} \right)$$

and multiplying by $\frac{d\bar{r}}{dt}$,

$$\frac{d\bar{p}}{dt} \cdot \frac{d\bar{r}}{dt} = -e \frac{d\bar{r}}{dt} \cdot \left[\frac{d\bar{r}}{dt} \times \bar{H} \right] = 0$$

Then since

$$\frac{d\bar{p}}{dt} \cdot \frac{d\bar{r}}{dt} = \frac{dm\bar{v}}{dt} \cdot \bar{v} = \frac{1}{m} \frac{d(m\bar{v})}{dt} \cdot m\bar{v} = \frac{1}{2m} \frac{d(m\bar{v} \cdot m\bar{v})}{dt}$$

therefore

$$\frac{1}{2m} \frac{d(mv)^2}{dt} = 0 \quad \text{and} \quad \frac{dv}{dt} = 0$$

The velocity is constant in the magnetic field, and all equations are relativistically valid.

Expressing the equation of motion in its three components,

$$\frac{m d^2 r}{dt^2} - m r \left(\frac{d\theta}{dt} \right)^2 = - e \frac{d\theta}{dt} \frac{\partial}{\partial r} (rA) \quad (1)$$

$$\frac{d}{dt} \left(m r^2 \frac{d\theta}{dt} \right) = e \frac{d}{dt} (rA) \quad (2)$$

$$\frac{m d^2 z}{dt^2} = - e r \frac{d\theta}{dt} \frac{\partial A}{\partial z} \quad (3)$$

Integrating (2)

$$m r^2 \frac{d\theta}{dt} = e r A + C' \quad (C' = \text{Const}) \quad C' = \frac{C}{e} \quad (4)$$

Taking the initial conditions $r = r_0$, $A = A_0$, $\frac{d\theta}{dt} = \left(\frac{d\theta}{dt} \right)_0$

Equation (4) can be expressed

$$\frac{m}{e} \left\{ r^2 \frac{d\theta}{dt} - r_0^2 \left(\frac{d\theta}{dt} \right)_0 \right\} = rA - r_0 A_0$$

or

$$\frac{m}{e} \frac{d\theta}{dt} = \frac{A}{r} + \frac{C}{r^2} \quad \text{where}$$

$$C = \frac{m}{e} r_0^2 \left(\frac{d\theta}{dt} \right)_0 - r_0 A_0$$

Inserting (4) in (1) and (3)

$$\frac{d^2 r}{dt^2} = - \frac{\partial Q}{\partial r} \quad \frac{d^2 z}{dt^2} = - \frac{\partial Q}{\partial z}$$

where

$$Q = \frac{e^2}{2m^2} \left(A + \frac{C}{r} \right)^2 = \frac{1}{2} \left(r \frac{d\theta}{dt} \right)^2 \quad (5)$$

then combining these equations we get

$$\left(\frac{dr}{dt} \right)^2 + \left(\frac{dz}{dt} \right)^2 = v^2 - 2Q = v^2 - \left(r \frac{d\theta}{dt} \right)^2 \quad (6)$$

In particular, for the case of the particle emitted from the center and moving on the plane of symmetry, then $C = 0$, $z = 0$, $dz/dt = 0$, and

$\partial A / \partial r = 0$ and the equation of motion becomes,

$$\frac{dr}{dt} = v^2 - \frac{e^2 A^2}{m^2} \quad \text{and} \quad mr \frac{d\theta}{dt} = eA \quad (7)$$

In order to have a spiral orbit, and the charged particle approach to a circle of radius $r = \rho$, the following conditions should be satisfied at $r = \rho$:

$$\frac{dr}{dt} = 0 \quad \text{and} \quad \frac{d^2 r}{dt^2} = 0$$

The first condition can be expressed as

$$v = \frac{eA}{m} \rho \quad (8)$$

and the second condition as

$$mv = e\rho H_{r=\rho}$$

From the relationships

$$\phi = \oint \bar{B} \cdot \bar{ds} = \oint \bar{A} \cdot \bar{dl}$$

it follows that

$$A_{r=\rho} = \frac{1}{\rho} \int_0^\rho H(r) r dr \quad (9)$$

and therefore

$$H_{r=\rho} \rho^2 = \int_0^\rho H(r) r dr \quad (10)$$

It might also be noted that from Equations (1), (8), and (9) the Vector Potential A is an extremum at $r = \rho$, i.e., $\left(\frac{\partial A}{\partial r}\right)_{r=\rho} = 0$ and in this case it is a maximum.

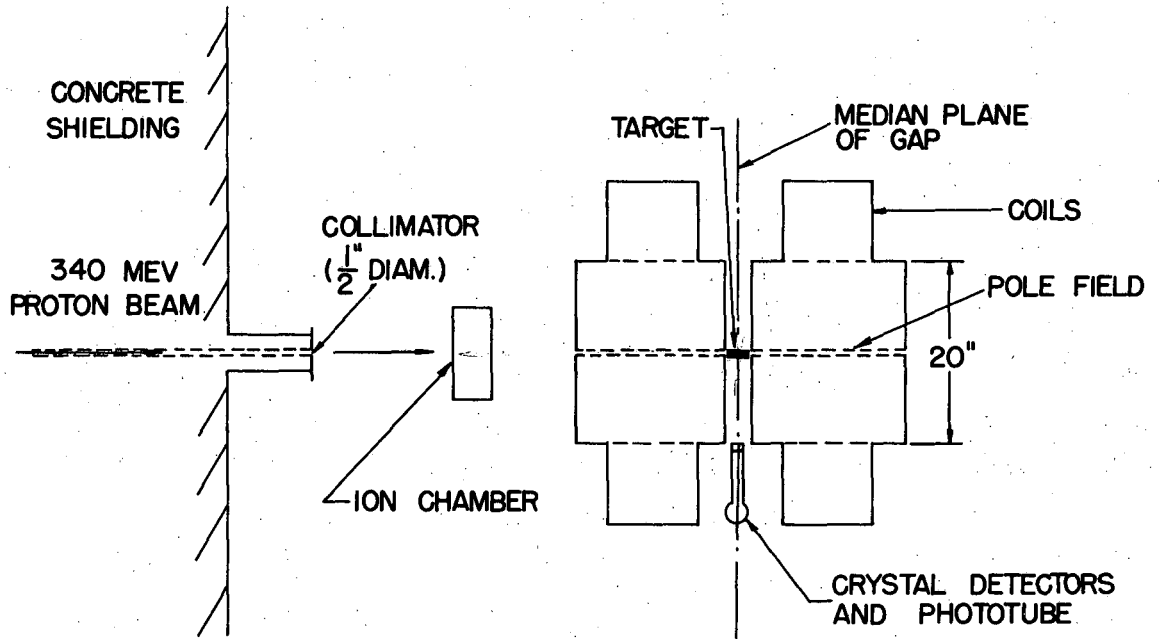
Therefore, as indicated by Iwata, Miyamoto, and Katani,¹⁰ Equations (8) and (10) are the definition of the stable orbit, and of the momentum of a charged particle in that orbit. A salient feature of this equation is the fact that the position of the stable orbit is determined by the shape of the magnetic field distribution, and is completely independent of the absolute magnitude of the field. (This is true as long as the

field shape does not change when H_{max} , i.e. the current setting, is changed. This requirement can usually be fulfilled.)

Examples of the field distributions employed are given in Figure 1. The B field distribution (associated with a 3-1/4-inch pole gap) was used in the early stages of the experiment. It has the advantage of quite large vertical focusing, with a resultant increase in the detection efficiency. The field distribution labeled A (associated with a gap of 2 5/8 inches) has practically no vertical focusing, as can be seen from the graph, except in the vicinity of the orbit. But it has the advantage of an $H\rho$ value at the orbit large enough to cover the upper end of the spectrum (> 50 Mev electrons). The presence of a homogeneous magnetic field in a major part of the gap also permits the employment of the proton moment nuclear fluxmeter for an accurate absolute calibration of the field.

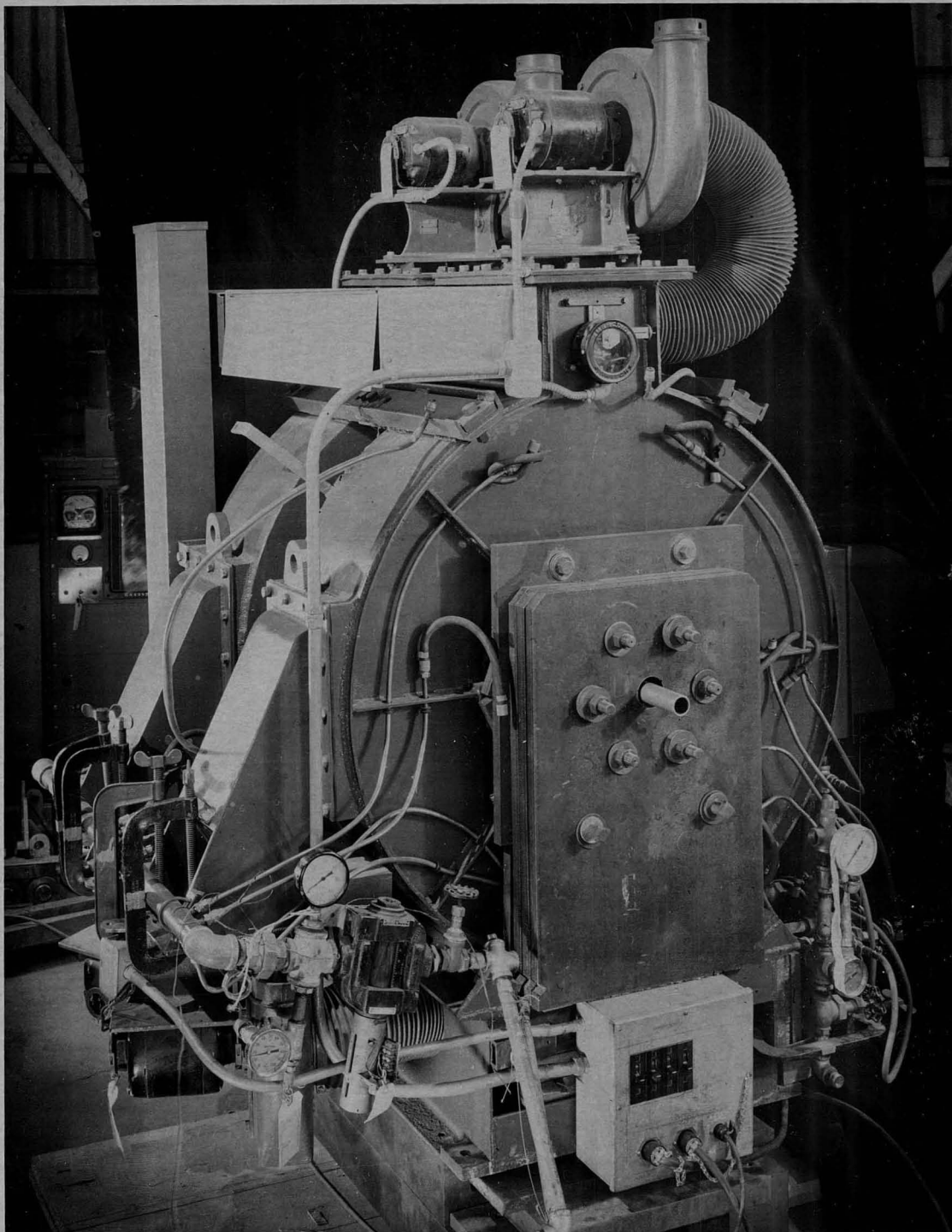
A plan view of the cyclotron, deflected beam, and positioning of the spectrometer is shown in Figure 2. The proton beam is collimated with a 4-foot long brass collimator of 1/2-inch internal diameter. The targets used were: Be 1-1/8-inch diameter x 3-1/4 inches long; C 1-inch diameter x 3 inches long; Al 1-inch diameter x 3 inches long. 1-1/4 inch holes were located in each of the pole pieces, coincident with the axis of the magnetic field, for the passage of the beam.

Figure 3 is a photograph of the spectrometer, and Figure 4 a close up view of the pole gap. The iron pole pieces were added, as were the iron bars and plates of the flux return path, in order to give an efficient shape to the field distribution in the gap, as well as to increase the absolute magnitude of the field and thus extend the upper energy limit of the spectrometer. Currents as high as 800 amperes were



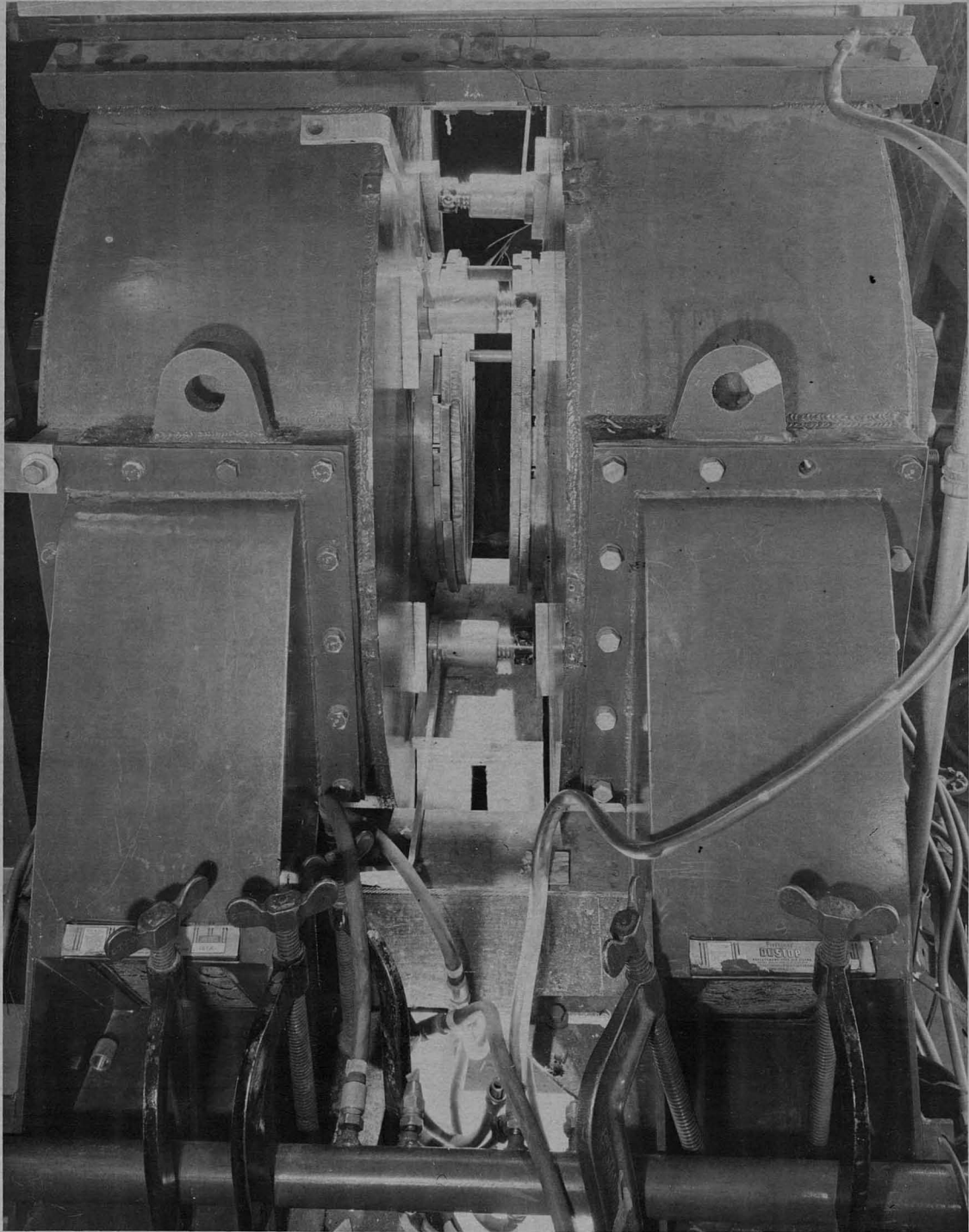
MU 18 08

Figure 2. Plan view of spectrometer in deflected beam of cyclotron.



SPIRAL ORBIT SPECTROMETER

FIG. 3



SPECTROMETER POLE GAP

FIG. 4

used with peak fields of about 20,000 gauss. The pole pieces are 20 inches in diameter, and the total weight of the spectrometer is about 4 tons.

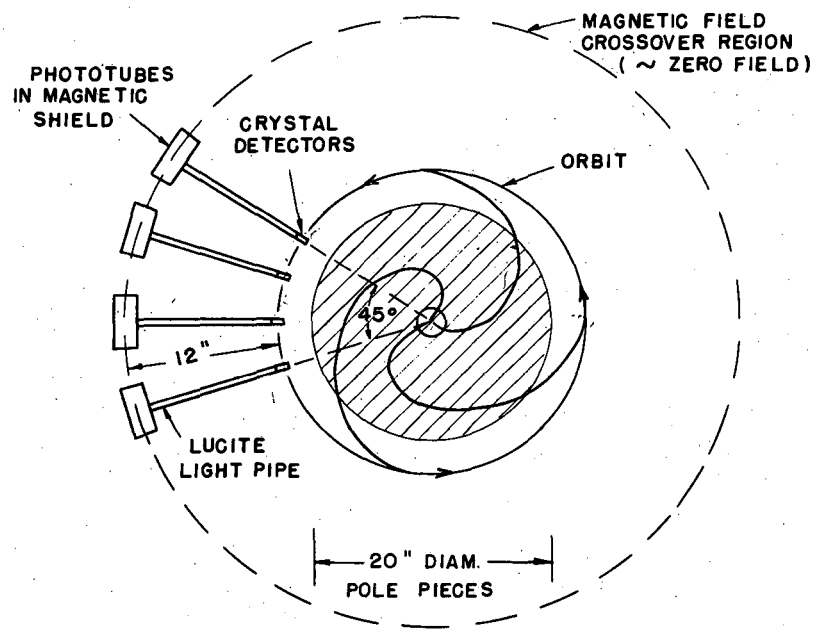
B. Scintillation Detection of Particles

For the detection of particles in the orbit, scintillation crystals and photomultiplier tubes were used. Figure 5 shows the arrangement of the detecting apparatus in the spectrometer. Quite clear anthracene crystals of dimensions $1 \frac{1}{4}$ inch x $\frac{3}{4}$ inch x $\frac{3}{16}$ inch were placed on one end of Lucite light pipes. Crystal and pipes were enclosed in reflecting aluminum foil, and the whole was wrapped with black tape. The photomultiplier tubes (1P21) were encased in a close-fitting magnetic shield of $\frac{1}{2}$ inch iron, slotted for insertion of the light pipe. These shields, as sketched in Figure 6, were effective in the somewhat large field gradients present at the flux cross-over region. Tests indicated that the phototube efficiency variation as a function of magnetic field setting was less than 3 percent over the entire range. The final crystal and phototube mount is shown in the photograph of Figure 7. Four crystal detectors were used, with a central angle of 15° between crystals. A particle moving in a straight line will be unable to traverse the four crystals.

C. Electronic Circuits

The electronic counting arrangement is presented in Figure 8. Signals from the phototube go into a discriminator and pulse former circuit (of resolving time 0.2μ sec.). At maximum sensitivity a 40 millivolt or larger pulse will trip these circuits and the output pulse is a uniform 30 volts. These pulses are then fed into a quadruple

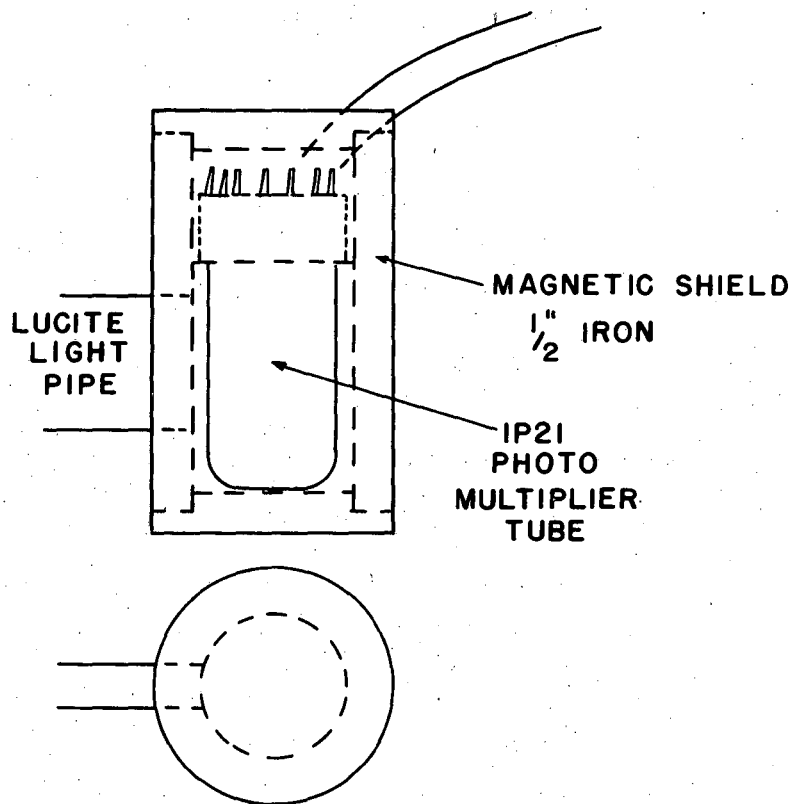
SPIRAL ORBIT SPECTROMETER
MEDIAN PLANE OF GAP



MU 1809

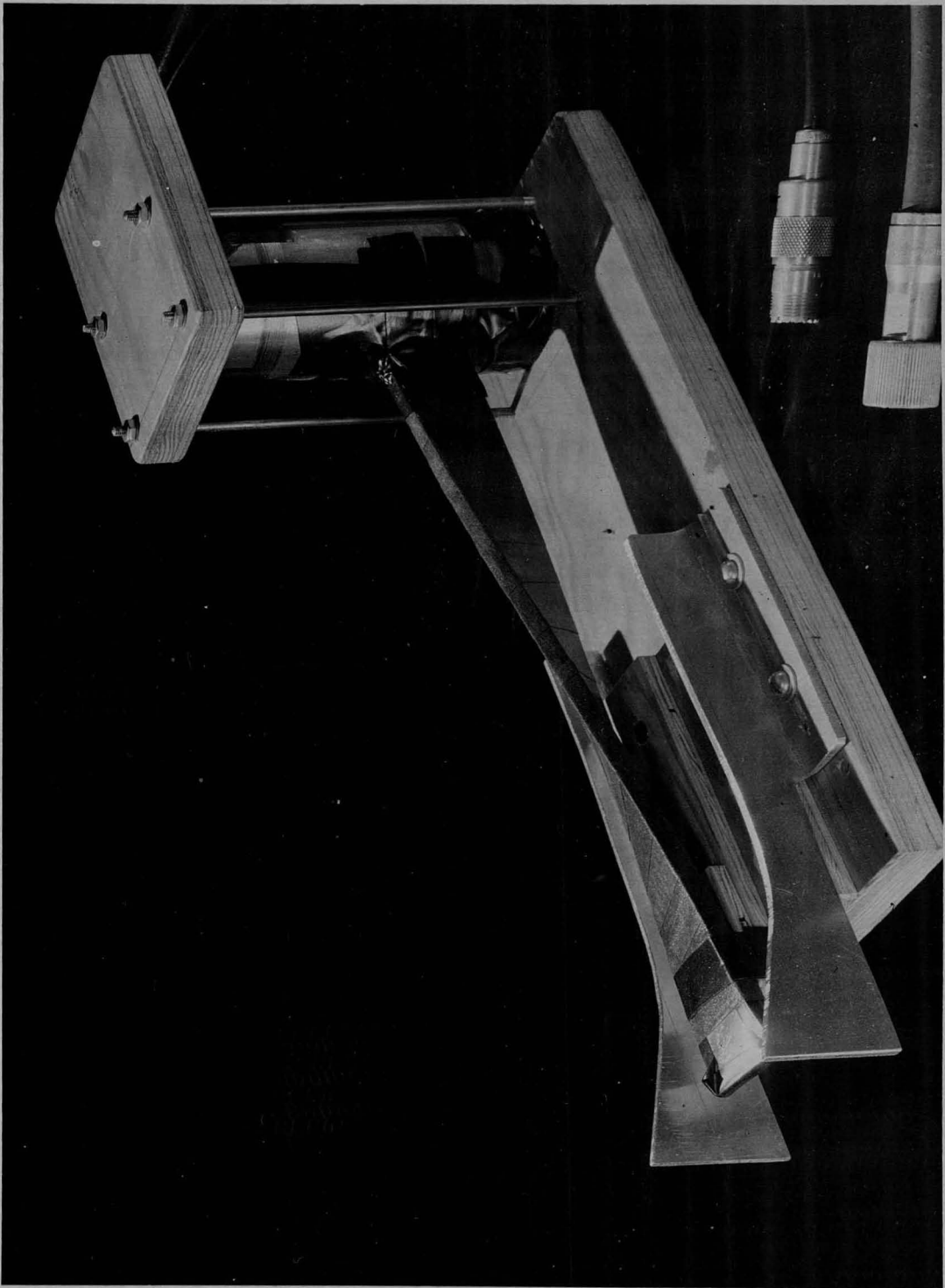
Figure 5. Spiral orbit spectrometer.

MAGNETIC SHIELDS
FOR PHOTO TUBE



MU 1810

Figure 6. Magnetic shield for phototube.



CRYSTAL AND PHOTOTUBE DETECTOR
FIG. 7

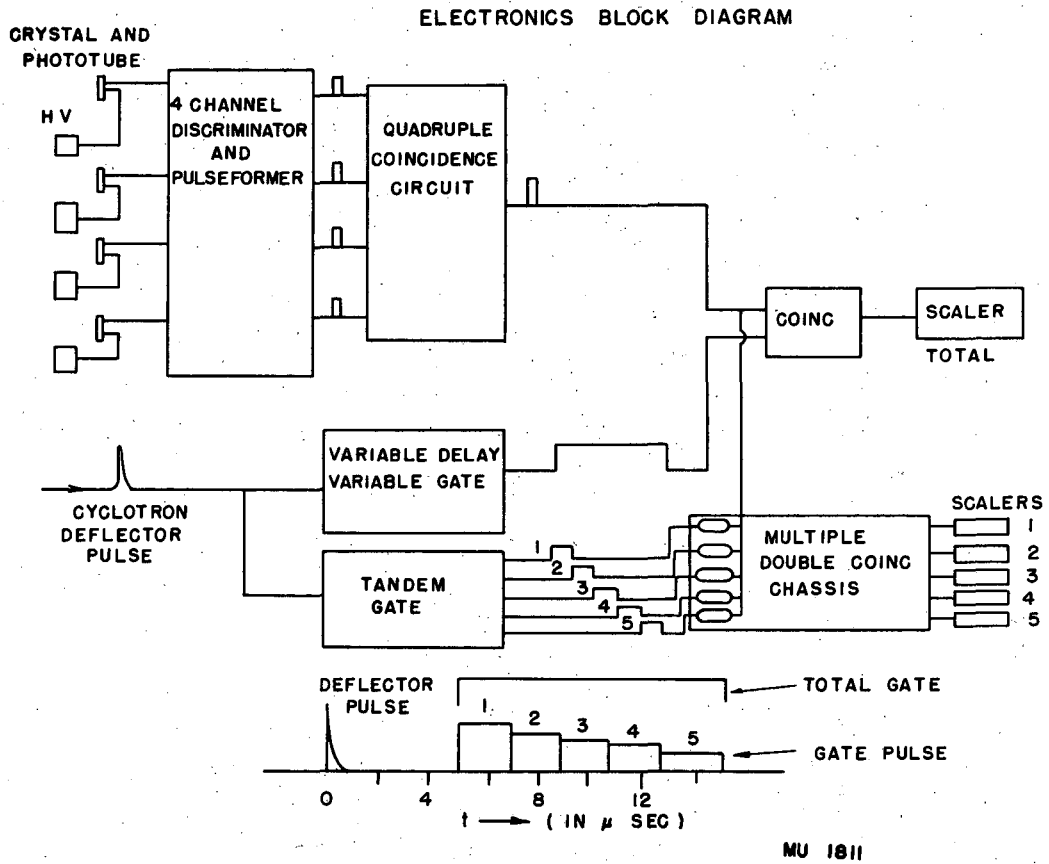


Figure 8. Electronics block diagram.

coincidence circuit (of resolving time $0.2 \mu \text{ sec.}$). The high voltage on the phototubes was usually in the vicinity of 1250 volts.

In order to identify these quadruple coincidences with the positions of μ^+ decay, it seems reasonable to require that they have the characteristic half-life. For this reason the quadruple coincidence signals are again fed into coincidence with $2 \mu \text{ sec.}$ gates so that the counting rate decay over $2 \mu \text{ sec.}$ intervals may be observed. The cyclotron beam has a repetition rate of ~ 60 pulses per second, and each pulse of the electrically deflected beam has a duration of less than $0.3 \mu \text{ sec.}$ The deflector pulse triggers the gate forming units. The position of the start of these tandem gates can be varied, and it was usually found desirable to delay the counting until about $5 \mu \text{ sec.}$ after the beam pulse. With a mean life of $2.15 \mu \text{ sec.}$, this obviously indicates a large loss in total counts obtainable. But the high singles counting rate during and immediately after the beam resulted in a rather high accidental quadruple background counting rate, which could be effectively eliminated only by the insertion of this delay.

The source of this large singles counting rate is not very well understood. A large neutron flux is known to exist in the shielded cave of the external beam port. Recoil protons and neutron induced activities are undoubtedly a major factor. Any intense short-lived γ activity of the target itself might contribute to accidental quadruples. In addition the disproportionately large signal due to the actual beam flux is occasionally capable of rendering the electronic detecting apparatus inoperative for several microseconds.

D. Background Determination

Several methods of determination of the background counting rate

were investigated, and the two most unambiguous methods are sketched in Figure 9. In the test labeled A, a 4-inch thick piece of lead -- large enough to completely cover the crystal, was placed in the orbit immediately above the top crystal. It did not block the crystals from any radiation from the target, nor in general from any other direction except that of the orbit. The test labeled B consisted of removing alternate crystals radially back out of the orbit 1 inch. The crystals were $3/4$ inch wide (dimension along the radius) so that this travel made it impossible for a particle in the orbit to give a quadruple coincidence. And yet the exposure of the crystals to all general background radiation was not diminished.

Because of the uncertainty of the source of the background, and the likely possibility that it would vary in an unknown manner with the counting rate of the particular part of the spectrum under observation, it was deemed necessary to reduce the background effectively to zero. The above tests were considered quite valid as to whether or not this condition was being met. As further assurance that the observed counts were real counts, another periodic check was made by observing the response of the counting rate as the cyclotron beam intensity was lowered by a factor of $1/2$ and $1/4$.

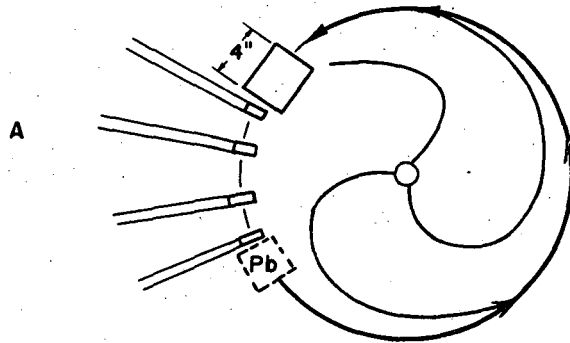
E. Operational Procedure

The integration of the cyclotron beam was accomplished by the use of an ion chamber coupled into an integrating electrometer.¹² The ion chamber was filled to 100 cm of Argon-CO₂ mixture, and was checked for linearity with beam intensity.

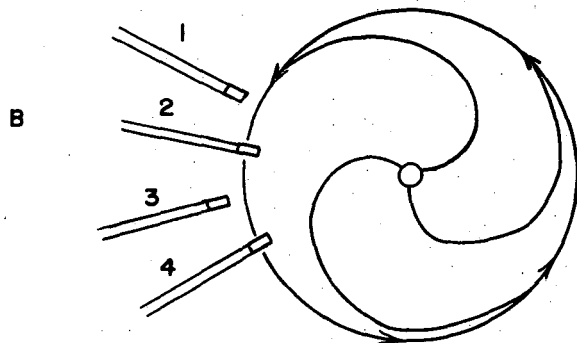
Under normal operating conditions the magnet current setting corresponding to a particular momentum interval would be maintained

¹² R. Aamodt, V. Peterson and R. Phillips, UCRL Report No. 526.

BACKGROUND TESTS



4" Pb IN PATH OF PARTICLES IN ORBIT



ALTERNATE CRYSTALS MOVED
1" OUT OF ORBIT

MU 1812

Figure 9. Background tests.

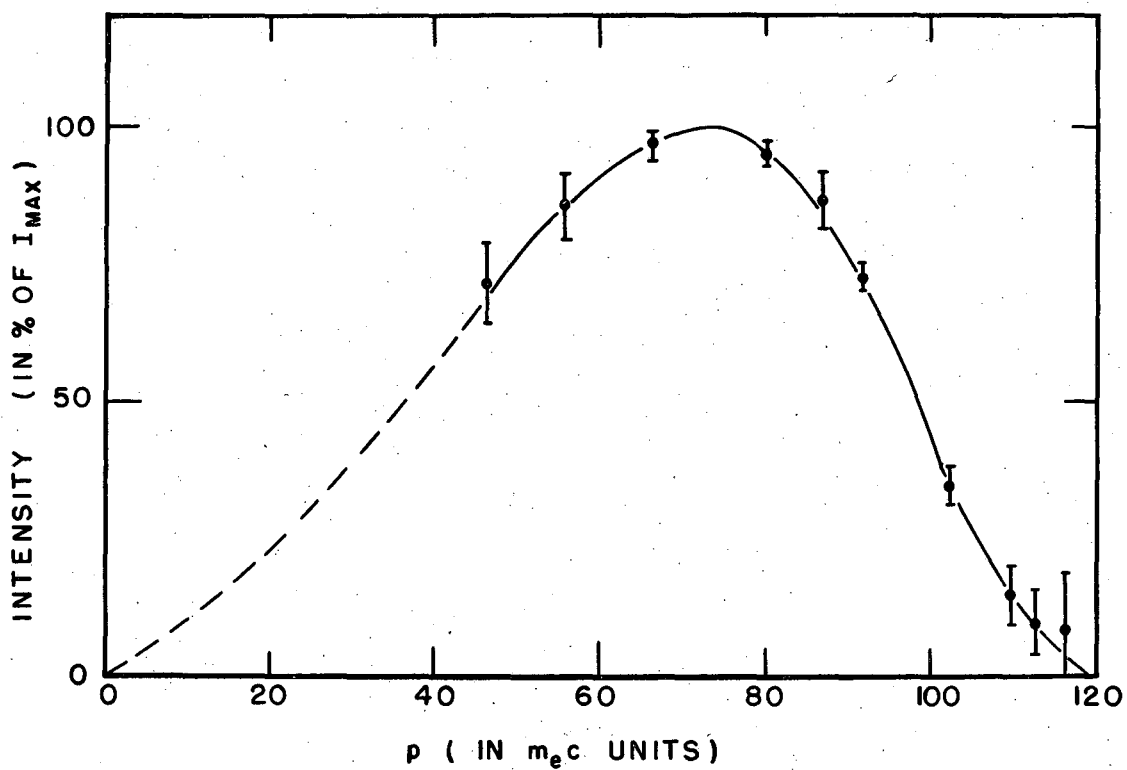
until a convenient charge was indicated on the electrometer. The exposure time would be of the order of 5 minutes. The electrometer was then cleared and a new momentum interval observed for the same total beam charge. In this manner the total momentum spectrum was covered in a relatively short period, and then the entire process would be repeated, usually about four times. This method served to eliminate long term drift effects as well as to permit a constant check on the reproducibility of the data. The background tests mentioned above would be conducted several times during the run.

III EXPERIMENTAL RESULTS

The results of the several experimental runs with the cyclotron are embodied in the graphs of Figures 10 and 11. In Figure 10 the experimental data are plotted as actually observed -- making only the initial correction of $I = \frac{I_{\text{OBSERVED}}}{H\rho}$ for a spectrometer. In Figure 11 these data have been corrected for the energy resolution peculiar to this instrument. The shape of the resolution curve is also included on the graph. A discussion of the accuracy of this correction is incorporated in the following section.

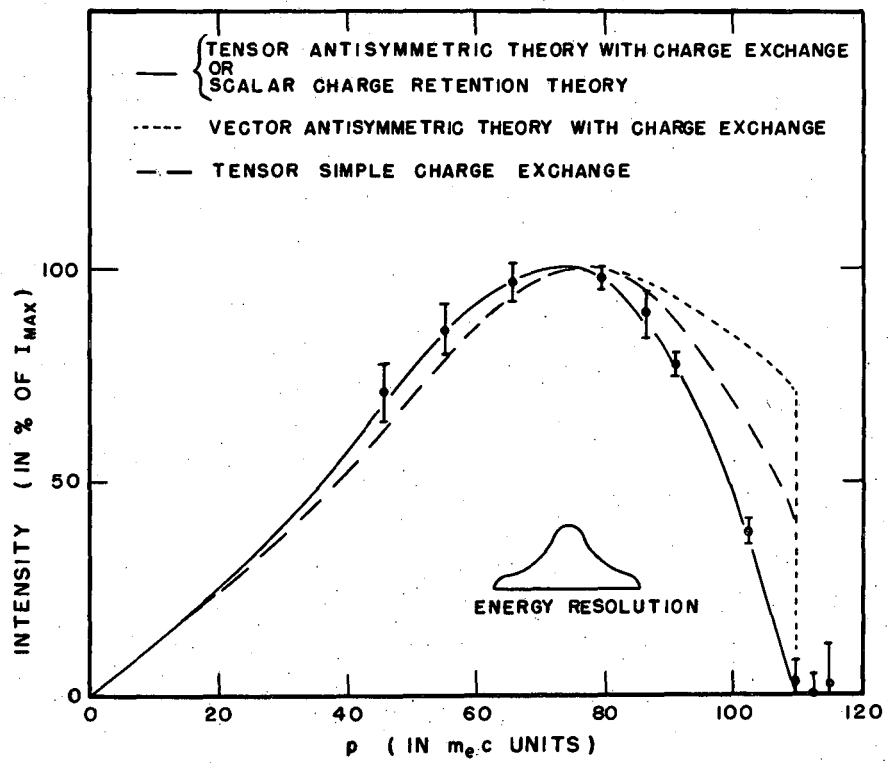
A total of about 4,000 counts were obtained for this spectrum determination. Some idea of the counting rate can be given by the data from a recent run wherein the counting rate, for a magnetic field setting corresponding to $p = 70 m_e c$, (momentum in units of electron mass times c) was in the vicinity of 7 counts/minute.

The agreement of the decay of the observed counting rate with that for μ^+ -meson decay is portrayed in Figure 12. All of the counts for the run considered are totaled for each successive gate and the counting rate given is the individual total for the respective gate. The slope of the line is arbitrarily drawn for $\tau_{\text{mean}} = 2.15 \mu \text{ sec.}$ as given by Nereson and Rossi.⁵



MU-1813

Figure 10. Experimental spectrum.



MU 1814

Figure 11. Corrected spectrum.

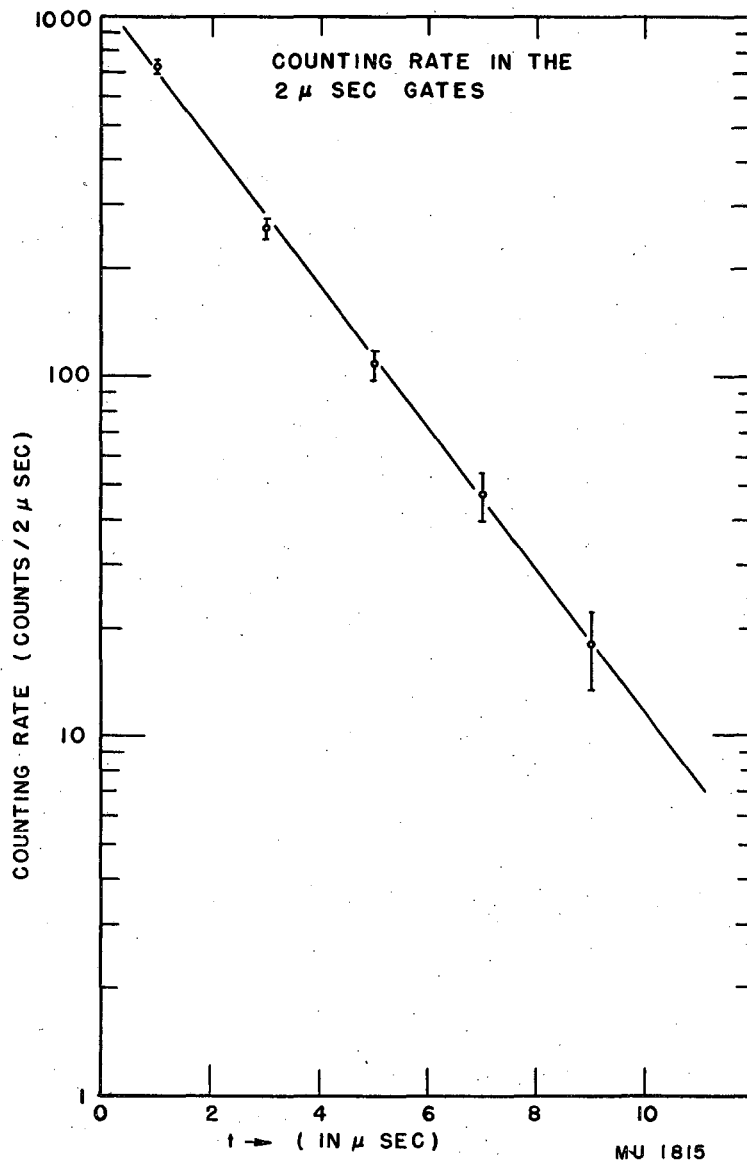


Figure 12. Counting rate decay curve, positron counting rate.

IV ACCURACY OF THE MEASUREMENTS

A. Magnetic Field and Orbit Determinations

The measurements of the absolute intensity of the magnetic field were done with a nuclear fluxmeter which is sufficiently accurate that the error in these determinations is negligible. The magnet current was adjusted by the use of a current regulator attached to the generator. Repetition of the measurements for the same setting of the magnet current has shown that the reproducibility is better than 1 percent. The change in field distribution against radius with different magnet currents was checked to be less than the error of the flip coil measurements which is of the order of ± 1 to 2 percent.

The position of the "stable orbit" was determined by numerical integration over the given field distribution. A systematic error may possibly exist in the evaluation of the momentum of the charged particles to be focused in the spectrometer. However the error is estimated to be no more than ± 1.5 percent from the absolute calibration and as for the relative value for any given set of magnetic fields the error should be less than 1 percent. It should be pointed out that if one can make the field distribution close to a $1/r$ dependence near the orbit, then the error in the evaluation of ρ by numerical calculation gives very little change in the $H\rho$ value.

B. Evaluation of Additional Background Effects

Other types of errors are also to be considered:

1. Very energetic beta-ray activity produced at the target.
2. Electrons from μ^- decay.
3. Superposition of positrons produced at the first crystal due to π^+ -mesons stopping in the first crystal and giving rise to $\pi^+ \rightarrow \mu^+$

decay and $\mu^+ \rightarrow e^+$ decay.

4. Effect of scattering of the electrons at the crystals and also during flight in 1 atmosphere pressure over a path length of 2 to 3 feet.
5. Effect of energy loss of the electrons going through matter both at the target, and at the crystals.

Fortunately, all these errors have been checked to be small in the region of the momentum spectrum, i.e. from 40 to 110 $m_e c$. The method of investigation of each effect was as follows:

1. Since the spectrometer is symmetric to charged particles of either sign, it is possible to have quadruple coincidences from negative particles of the same momentum as that of the positrons under observation. Therefore any beta activity in this momentum range would give rise to real counts. However, theoretical considerations indicate that beta activity with a beta energy > 20 Mev is extremely unlikely. Owing to the difficulty of measurement there is not much experimental data on this subject. It is apparent, however, that our experimental arrangement was simultaneously a feasible method of making such an investigation. The magnitude of such possible contamination was shown to be quite small by these tests:
 - a) by counting with reduced energy of the proton beam. The yield of π^+ mesons is supposed to be very sensitive to the proton energy¹³ while the beta-ray activity is expected to be about the same, i.e. relatively independent of the proton energy in the region of 300 to 340 Mev.
 - b) by counting with targets of different elements. The energy spectra for Be, C, and Al were almost the same, and one would

¹³ S. Jones and S. White, Phys. Rev. 78, 12 (1950)

expect that the energies and intensities of any contaminating beta activities would be quite sensitive to the target element.

2. Again because of the acceptance of the spectrometer of both + and - charged particles any $\mu^- \rightarrow e^-$ decay would be included in with the $\mu^+ \rightarrow e^+$ decay. Of course because of the large capture probability of the π^- in the target material this effect was expected to be quite small. This fact was corroborated by placing a 4-inch Pb absorber below the bottom crystal, (similar to the background test discussed earlier as applied to the top crystal) and the relatively small change in the counting rate could be accounted for by the slight decrease in the transmission solid angle of the spectrometer.
3. Effect of π^+ stopping and decaying in the first crystal. It should be noted that the spectrometer focuses π -mesons of a corresponding H_p . Indeed, this property was employed in an earlier experiment for a determination of the π^+/π^- ratio in a single emulsion.¹⁴ The π^+ energy corresponding to an H_p of $p = 100 m_e c$ is 12 Mev. Approximately 1.2 gm/cm^2 of Cu will stop these mesons, and such an absorber was placed in the orbit about 8 inches from the first crystal. Any real counts due to this source would drop off by approximately the ratio of the solid angle subtended by the crystals for the old and new positions of the meson absorber. The counting rate change was slight, so evidently the original small solid angle kept this effect small.
4. Scattering of electrons. This was tested by putting an additional crystal, $7/8$ inch thick in front of the first one. It is calculated that this will exaggerate the scattering by a factor of three. The counting rate indicated however that even this accentuated

¹⁴ R. Sagane and P. Giles, Phys. Rev. 81, 653A (1951)

effect is quite small, so that the actual effect of scattering in the regular crystals should not be an important factor. The pole gap enclosure was not evacuated so that the average 2 or 3 foot trajectory of the particle was through that amount of normal atmosphere. The long path magnifies the effect of the scattering, but the small amount of matter traversed ($\sim 0.03 \text{ gm/cm}^2$) together with the particle energies involved ($\sim 35 \text{ Mev}$) are the basis for the estimate that the air scattering is less than that in the crystals which was tested to be small.

5. Energy loss in crystals and in target. The energy loss due to ionization per crystal is calculated to be close to 0.8 Mev over the momentum range considered. The main effect of this loss is the tendency for the particle to leave the orbit due to the lowered momentum. However, this momentum change is relatively small, (for a 40 Mev positron, this corresponds to a 2 percent momentum change). Moreover, since this energy loss per crystal is relatively constant for a 30-50 Mev positron, the net effect of this momentum shift will be a slight decrease in the detection efficiency which will not change the shape or position of the spectrum. The mean radiation losses over this momentum range for carbon, (main constituent of the scintillation crystals) is less than 1/5 the ionization losses so this effect can be considered as negligible.

Energy losses in the target, though, are more important, The mean thickness of target material traversed by the positrons is calculated by considering: 1) the efficiency of the spiral orbit spectrometer for sources made up of cylindrical shells of varying radii, and 2) the radial density distribution of μ^+ decay in the

target. For the case of a beryllium target, the radiation loss compared to the ionization loss is relatively smaller than for the case of carbon mentioned above. These considerations lead to an estimate of 0.25 inch as the mean target thickness traversed with an overall average energy loss of 2 Mev. This correction is included in both spectrum plots.

6. Miscellaneous sources. As for the electrons due to the γ -rays produced, by capture of π^- or π^0 decay, these are eliminated by starting the counting only after a delay of several microseconds. The percentage of π^+ -mesons which decay directly into positrons is extremely small,¹⁵ and any such positron counts are similarly eliminated by the use of delay gate circuits.

C. Resolution Curve of Spectrometer

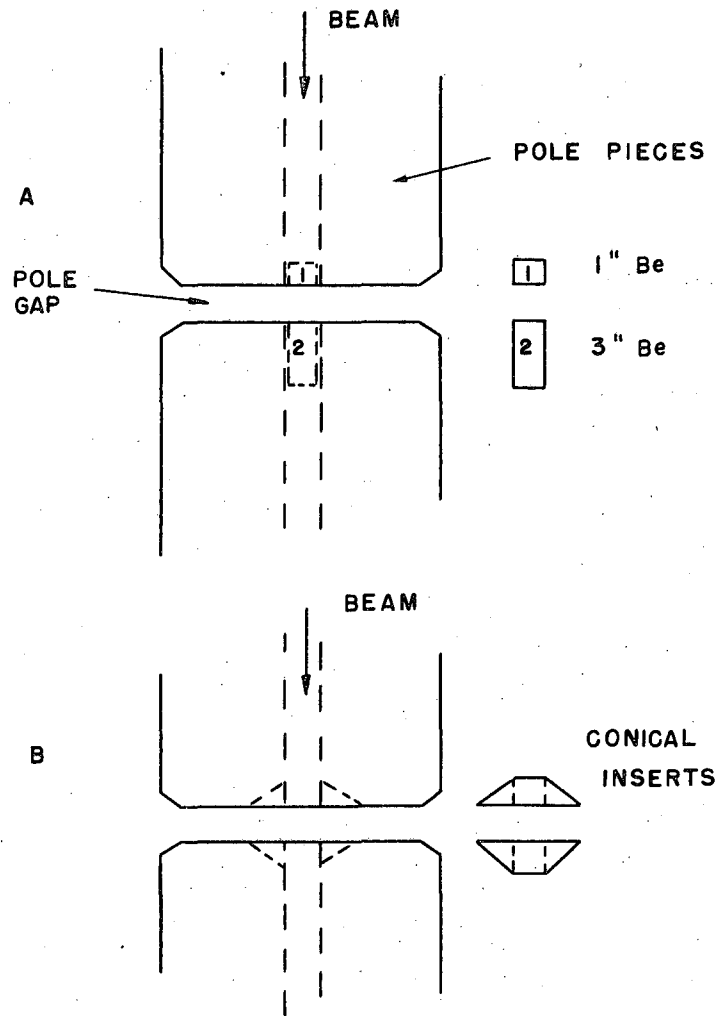
One of the most important points that should be discussed here is the resolution curve of the spectrometer. There will be a spread in the resolution curve due to the effect of the comparatively large diameter of the target and also added to this will be the electron contribution of the pole surfaces. This latter effect may be appreciable, especially in the region close to the axis because the density of π -mesons absorbed in this region is expected to be rather high. The π -mesons thus absorbed may result in a moderate electron emission from the pole surfaces.

The ratio of the target radius to the radius of the critical orbit should be less than 0.03, and for maximum energy resolution as low as 0.01. In order to obtain a reasonable counting rate a rather large target was used for which the ratio was 0.05. However, the effective

¹⁵ H. Friedman and J. Rainwater, Phys. Rev. 81, 644 (1951)

ratio is smaller than this due to the collimation which results in a higher beam density at the center of the target. The ratio should be close to 0.04, and for the detector system used, this corresponds to an energy resolution of about 10 percent. The resolution of the spectrometer is rather sensitive to the central angle subtended by the detector system. In this apparatus the angle was 45° which is sufficiently large that it helps to offset the spread due to the large diameter target. The ratio of crystal detector width to the radius of the orbit is $1/15$. The energy resolution is relatively insensitive to the crystal width in this region (e.g. a 50 percent increase in detector width would affect the energy resolution less than 10 percent). Since an increase in the crystal width would increase the overall detection efficiency, such a possibility had been considered. But the drop in light collection efficiency for such a crystal would probably offset most of this gain.

In order to study the spread due to electrons from the pole surfaces, two tests were conducted, as sketched in Figure 13. In the test labeled A, two Be targets were employed, both of $1\frac{1}{8}$ -inch diameter. The first one, 1 inch long, was positioned such that it was forward of the gap with its rear surface flush with the gap. The second one, 3 inches long, was back of the gap, and with its front surface flush. With this arrangement the number of mesons absorbed by the pole piece surfaces in question is estimated to be of the order of $1/2$ of normal, and of course the counts due to electrons from the target will be completely missing. The test labeled B consisted of taking data with the target in its normal position and with removable cones as shown, first in position -- and then with them completely out



MU 1816

Figure 13. Pole surface background.

of the gap. The electron contribution of the pole pieces should be considerably decreased by the absence of these particular pole surfaces. The information obtained from these tests is that the background counts due to this effect of the pole surfaces is less than 1/10 of the total area of the resolution curve.

The proton beam density at the target is also an important factor in the shape of the resolution curve. The usual beam collimator employed was 4 feet long and 1/2-inch internal diameter. This resulted in a fairly homogeneous beam of 3/4 inch at the target, and considerable time was always given for the precise adjustment of this beam on the target center. This gives a denser population of π -mesons close to the axis of the 1 1/8-inch diameter target which tends to diminish the otherwise expected resolution spread. So from the combined results of both calculations and tests mentioned above the resolution curve as given in Figure 11 is considered to be the most likely one.

The corrections due to this resolution curve are very small for the momentum spectrum around the intensity maximum, but are large for points close to the momentum maximum. So it might be pointed out that the error in the estimation of the resolution curve does not affect the momentum value of I_{\max} over 1 to 2 percent -- but may affect the momentum value of E_{\max} about 3 to 4 percent.

V MESON DECAY PROCESS AND OUTLINE OF MESON THEORIES

The nature of the μ -meson and its decay products are discussed in some detail in Tiomno, Wheeler, and Rau,¹⁶ and more recently by Michel.¹⁷ As stated earlier, the decay process $\mu^+ \rightarrow e^+ + 2\nu$ is the favored reaction, for the following reasons.

Meson decay processes resulting in two emitted particles, for example,

$$\mu^+ \rightarrow e^+ + \text{neutrino}$$

$$\mu^+ \rightarrow e^+ + \text{photon}$$

$$\mu^+ \rightarrow e^+ + \mu_0 \text{ (neutral meson)}$$

would yield a line spectrum for the electron energy, and are thus inconsistent with observation. Processes yielding four or more decay particles are also untenable because the mean energy of the positron in such a process would be only 1/4 of the μ -meson rest mass energy or less, and this is contradicted by observed spectra.

The three particle decay process is therefore most logical. Three electron emission is excluded by cloud chamber evidence. Absorption experiments rule out the emission of photons. Therefore

$$\mu^+ \rightarrow e^+ + \text{neutrino} + \mu_0 \text{ (neutral meson of spin } 1/2)$$

or the special case where

$$\mu_0 \rightarrow \text{neutrino}$$

$$\mu^+ \rightarrow e^+ + 2\nu \text{ are the favored processes.}$$

But the reaction yielding a neutral meson results in a positron spectrum which has its maximum intensity shifted toward the high momentum limit. In addition, there is a corresponding lowering of the

¹⁶ J. Tiomno, J. Wheeler, and R. Rau, Rev. Mod. Phys. 21, 144 (1949)

¹⁷ L. Michel, Proc. Phys. Soc. England, 63, 514 (1950)

positron momentum maximum for heavier assumed masses of the neutral meson. This latter effect is large enough that any neutral meson mass greater than $20 m_e$ is incompatible with the observed spectrum. The former effect, that of a shift of the intensity maximum towards higher momentum values, is still a useful index for assumed values of the μ_0 mass of less than $20 m_e$. And comparison of these curves with the observed spectrum indicates that while a finite neutral meson mass cannot be ruled out, the most likely case is that of zero mass. Therefore, a highly probable and also simple process is the $\mu^+ \rightarrow e^+ + 2\nu$ decay scheme.

Beta decay theory is applicable to both nuclear beta decay and to μ -meson decay. The five simple forms of coupling: scalar, pseudoscalar, vector, pseudovector, and tensor are investigated by Tiomno, Wheeler, and Rau, and the theoretically expected curves for μ -meson decay are presented. The choice of the form of coupling has a noticeable effect on the shape of the positron energy spectrum. This is not true in nuclear beta decay. This is a relativistic effect and arises because the recoil momentum of the positron is taken up not by a residual nucleus, as in nuclear decay, but by small or zero rest mass particles which must therefore travel close to or at the velocity of light.

As in beta decay, it is convenient for the mathematical treatment to adopt the convention that the meson decay process be represented as the destruction of two particles, and the creation of two other particles. Thus the process

$$\mu^+ \rightarrow e^+ + 2\nu$$

may be described as

$$\mu^+ + e^- \rightarrow \nu + \nu$$

or

$$\mu^+ + \underline{\nu} \rightarrow e^+ + \nu$$

where the underline denotes a negative energy state.

There are several ways to describe each of the decay processes resulting from a study of a particular one of the five forms of coupling listed above. Because the end products are all light particles, there is no way to decide whether the μ^+ goes into a neutrino, or a positron. And for the case of creation of two identical neutrinos, the antisymmetry of the wave function must be taken into account. When all of the various alternatives are considered, it can be shown that each is equivalent to one or the other of the following possibilities, as shown in Table I. (A $\mu^+ \rightarrow \nu$ is considered an exchange of charge, whereas a $\mu^+ \rightarrow e^+$ is not.)

Table I

Description of $\mu^+ \rightarrow e^+ + 2\nu$	Exchange of charge	Nature of neutral particles	Name used to describe theory
$\begin{pmatrix} \mu^+ \\ e^- \end{pmatrix} \rightarrow \begin{pmatrix} \nu \\ \nu \end{pmatrix}$	Yes	Identical Neutrinos	Antisymmetrical charge exchange
$\begin{pmatrix} \mu^+ \\ \nu \end{pmatrix} \rightarrow \begin{pmatrix} \nu \\ e^+ \end{pmatrix}$	Yes	Neutrino Anti neutrino	Simple charge exchange
$\begin{pmatrix} \mu^+ \\ \nu \end{pmatrix} \rightarrow \begin{pmatrix} e^+ \\ \nu \end{pmatrix}$	No	Neutrino Anti neutrino	Charge Retention

Each of the five simple forms of coupling will then yield three different energy spectra, corresponding to each of the three alternatives listed above. It should be pointed out that there is no theoretical objection to a linear combination of the different forms of coupling.

VI CONCLUSIONS

The momentum spectrum obtained is shown in Figures 10 and 11. The momentum value for the intensity maximum is $p = 74 \pm 3 m_e c$. The momentum maximum is $p = 110 \pm 5 m_e c$. For a μ decay scheme of $\mu^+ \rightarrow e^+ + 2\nu$, and assuming the neutrino mass $\cong 0$, then the μ -meson mass corresponding to this momentum maximum is $220 \pm 8 m_e c$.

In an examination of the experimental spectrum as compared to the theoretical curves¹⁶ for simple types of coupling, the following conclusions can be drawn. Of the 15 theoretical interactions (different interactions occasionally yield similar curves so that the number of distinct spectra is less than 15) all but 4 may be rejected quite completely.¹⁸ The four remaining are

- (1) Tensor, antisymmetric with charge exchange
- (2) Tensor, simple charge exchange
- (3) Scalar, charge retention
- (4) Pseudo scalar, charge retention

The curves resulting from interactions (1), (3), and (4) are identical and in good agreement with the observed spectrum, as shown in Figure 11. Due to the breadth of the energy resolution curve (as shown in Figure 11) the interaction (2) above still retains a certain probability. The agreement of this theoretical curve with the observed spectrum is sensitive to the actual μ -meson mass. That is, calculations indicate that while for a meson mass of $m_\mu = 220 m_e$ interaction (2) has negligible probability, this probability increases with decreasing meson mass until for the case of $m_\mu = 210 m_e$, its agreement with the data is 0.7 as probable as that of the theories (1), (3), and (4).

¹⁸ T. Green, Private communication

This simultaneously defines the probability of a finite upper limit for the spectrum. That these possibilities are to be considered is emphasized by a recent determination of the μ -meson mass by Birnbaum, Smith, and Barkas¹⁹ of $m_{\mu} = 210 \pm 2 m_{e.c.}$

By combining several of the simple types of coupling, theoretical spectra result which range over wide latitudes. Therefore if complex combinations of more than one of the interactions are to be considered possible, then the experimental curve will still leave a considerable amount of ambiguity in the identification of the combination.

An examination of the data of previous investigators with reference to the results of this experimental study enable these comparisons to be made: The work of Steinberger,⁷ while containing a large total number of events, suffers from the various contributions to range straggling. The data does not permit a positive indication of the presence of a continuous spectrum, as opposed to several unique energies. The upper limit of the spectrum is rather indeterminate. The investigation of Davis, Lock, and Muirhead,⁹ gave indication that a continuous spectrum was quite likely. Only 81 tracks were studied though, and scattering fluctuations resulted in calculated decay electron energies as high as 70 Mev, which appear considerably too high. The cloud chamber data of Leighton, Anderson, and Seriff⁸ enable them to make a meson mass determination of $217 \pm 4 m_{e.c.}$ They obtained only 75 tracks though, and these, portioned out over the range of the spectrum, result in a large statistical error in the spectrum.

The present work then has resulted in a much more accurate spectrum. Moreover, the technique of the measurement, the employment of

¹⁹ W. Birnbaum, F. Smith, and W. Barkas, to be published

the spectrometer and counter detection methods, is an interesting contribution to the experimental study of this problem.

VII ACKNOWLEDGMENTS

It has been a privilege to work with Prof. Ryoichi Sagane on this problem. His contributions on all phases of the experiment are very much appreciated. Dr. Walter Barkas originally pointed out the possibility of this application of the spectrometer and his continuing interest helped overcome the early difficulties. Mr. Harmon Hubbard contributed many helpful discussions, and a considerable amount of time. Thanks are due to Mr. Duane Sewell and his group for their nuclear fluxmeter measurements, and to Prof. Powell for his extended loan of the Helmholtz coils. The assistance of Mr. Peter Giles on the magnet and generator adjustments is appreciated, as is the cooperation of J. Vale and the cyclotron crew.

The interest of Prof. Ernest O. Lawrence in this research is appreciated, particularly as regards the circumstances which resulted in the availability of the spiral orbit spectrometer. The author is indebted to Prof. Burton Moyer for his suggestion that this work be undertaken and for his evaluation of the report.